

Increased capillary tortuosity and pericapillary basement membrane thinning in skeletal muscle of mice undergoing running wheel training

Oliver Baum¹, Carole Sollberger^{2*}, Andrea Raaflaub^{2*}, Adolfo Odriozola²,
Gunnar Spohr¹, Sebastian Frese¹, and Stefan A. Tschanz²

¹ Institute of Physiology, Charité-Universitätsmedizin Berlin, Berlin, Germany

² Institute of Anatomy, University of Bern, Bern, Switzerland

* Carole Sollberger and Andrea Raaflaub contributed equally to this paper

Key words: capillaries, endurance exercise, mouse, morphometry, skeletal muscle, transmission electron microscopy

Author for correspondence:

Dr. Oliver Baum

Institute of Physiology

Charité-Universitätsmedizin Berlin

Charitéplatz 1

D-10117 Berlin

Germany

e-mail: oliver.baum@charite.de

ABSTRACT

To work out which microvascular remodeling processes occur in murine skeletal muscle during endurance exercise, we subjected C57BL/6-mice to voluntary running wheel training for 1 week (1wk-t) or 6 weeks (6wks-t). By means of morphometry, the capillarity as well as the compartmental and sub-compartmental structure of the capillaries were quantitatively described at the light microscopy and at the electron microscopy level, respectively, in the plantaris muscle (PLNT) of the exercising mice in comparison to untrained littermates. In the early phase of the training (1wk-t), angiogenesis (32%-higher capillary-fiber (CF)-ratio; $P<0.05$) in PLNT was accompanied by a tendency of capillary lumen enlargement (30%; $P=0.06$) and reduction of the pericapillary basement membrane thickness (CBMT; 12.7%; $P=0.09$) as well as a 21%-shortening of intraluminal protrusion length ($P<0.05$), all compared to controls. After long-term training (6wks-t), when the mice reached a steady state in running activity, additional angiogenesis (CF-ratio: 76%; $P<0.05$) and a 16.3%-increase in capillary tortuosity ($P<0.05$) were established, accompanied by reversal of the lumen expansion (23%; $P>0.05$), further reduction of CBMT (16.5%; $P<0.05$) and additional shortening of the intraluminal protrusion length (23%; $P<0.05$), all compared to controls. Other structural indicators such as capillary profile sizes, profile area densities, perimeters of the capillary compartments and concentrations of endothelium-pericyte peg-socket junctions were not significantly different between the mouse groups. Besides angiogenesis, increase of capillary tortuosity and reduction of CBMT represent the most striking microvascular remodeling processes in skeletal muscle of mice that undergo running wheel training.

INTRODUCTION

In particular, two tissues/organ systems perceive the systemic impact provoked by regular physical activity (such as running or cycling training) that might significantly improve physical fitness and thus positively influence the quality of life, including extension of lifetime. First, endurance exercise triggers adaptive changes in the structure and function of the skeletal muscle fibers, i.e. by mitochondrial biogenesis (Holloszy, 1975; Hood et al., 2006) and by induction of fiber type shifting without hypertrophy (Pette and Staron, 1997). Most molecular mechanisms that have been identified up to now to contribute to physiological responses to endurance exercise are attributed to skeletal muscle fibers (Hoppeler et al., 2011). Second, a significant proportion of the positive effects evoked by regular physical activity are related to the cardiovascular system (Hellsten and Nyberg, 2016). In particular, the heart and larger-sized blood vessels may functionally adapt to endurance exercise and thereby contribute to health improvements (Hellsten and Nyberg, 2016; Laughlin, 2016). However, it also appears likely that the capillaries as the unit of the vascular system with the smallest diameter may undergo microvascular remodeling in response to a continuous training stimulus. Consequently, the microcirculation may supply peripheral tissues with oxygen and nutrients and may remove carbon dioxide and catabolic products, respectively, in a more efficient way.

The most prominent example for such an endurance exercise-induced microvascular remodeling analyzed so far is the increase in the numerical density of the capillaries, which is a process being designated angiogenesis (Hudlicka, 1998; Olfert et al., 2016). Other adaptive changes of the capillary system structure in skeletal muscles in response to endurance exercise (or chronic electrical stimulation, an animal model which resembles endurance exercise) have hitherto only been described sporadically, such as pericapillary basement membrane thickness (CBMT) reduction (Baum and Bigler, 2016; Williamson et al., 1996) as well as transient short-term EC thinning (Peeze Binkhorst et al., 1989) and late-stage endothelial cell (EC) swelling (Egginton and Hudlicka, 1999). A systematic synopsis of the structural adjustments of skeletal muscle capillaries to endurance exercise still needs to be performed.

In order to understand the dynamics of microvascular remodeling in response to endurance exercise, it is helpful to regard the regulation of the capillary system phenotype to fulfill its carrier function as a negative feedback control circuit. According to this cybernetic concept, the system is represented by the capillary

function as exchanger, the sensor is denoted by several molecular systems and the controller is given by the capillary phenotype. For understanding this concept, it is helpful to consider some molecular players that have already been identified to operate in such negative feedback control circuits. If the microcirculation is not sufficiently structured to fulfill the metabolic demands imposed on the musculature (e.g. during/after endurance exercise), the oxygen partial pressure reduces and/or the concentrations of energy substrates or carriers become too low. The dysfunction is sensed by ECs and/or the muscle fibers (e.g. by the prolyl-4-hydroxylase domain (PHD) proteins/hypoxia-inducible factor (HIF) oxygen sensing system; 5'-AMP-activated protein kinase (AMPK), sirtuins (SIRT6), peroxisome proliferator-activated receptors (PPARs), soluble guanylate cyclase (sGC) (for overview; see (Freysenet, 2007; Hoppeler et al., 2011)). This information is subsequently converted into an altered gene expression profile (control variable; e.g. by changing the activity levels of the molecular AMPK/PGC-1 α /VEGF axis (Leick et al., 2009)), which then alters the EC phenotype (downstream output). If the metabolic homeostasis is re-established, the adjustment of the capillary phenotype is not continued or might be reversed. This model demands that the structural phenotype of the capillary system in skeletal muscle is tightly regulated and its plasticity is relevant for the correct function of the muscular tissue according to the basic demand of biology 'function follows form' adjusted without designer. We therefore consider it crucial to exactly understand the mechanisms of how the phenotype of the capillary system is formed at different stages of the adaptive process to endurance exercise activity.

Recently, we have characterized the ultrastructure of capillaries in skeletal muscle of humans before and after an 8-week period of endurance exercise (Baum et al., 2015). The intense ergometer training of the study participants was accompanied by angiogenesis in the vastus lateralis muscle (VL) biopsies, which was statistically related to increased microcirculatory pericyte (PC) coverage and thinning of CBMT (Baum et al., 2015). We furthermore observed a significant volume expansion of the capillary endothelial cells in the muscle biopsies, which was not related to the onset of angiogenesis (Baum et al., 2015). However, these findings represent only end-stage observations and do not provide information about early adaptive responses of the capillaries to the training stimulus.

In continuation of this previous investigation performed on human skeletal muscle biopsies (Baum et al., 2015), we have now assessed whether the structure of

skeletal muscle capillaries is likewise changed in mice exposed to endurance training. In particular, we hypothesized that the structural changes of the capillary organization in skeletal muscle of mice are 1. similar to those in humans after a long period of endurance training and 2. already manifested in early stages of the training. To verify these hypotheses, we have now subjected C57BL/6 mice to voluntary running wheel training for 1 week (1wk-t) or 6 weeks (6wks-t) and quantitatively described the capillarity in the plantaris muscle (PLNT) as well as the compartmental and sub-compartmental organization of capillaries in comparison to that of untrained control mice.

MATERIALS AND METHODS

Animals

Eighteen male C57BL/6J mouse (*mus musculus*) littermates in the age of 12 weeks (purchased from Charles River, Sulzfeld, Germany) were randomly allocated to one of three groups: (1) sedentary control mice; (2) mice trained for 1 week (1wk-t) and (3) mice trained for 6 weeks (6wks-t).

All mice were maintained in a conventional animal facility in Bern with a fixed 12-h light/dark cycle on a commercial pelleted chow diet with free access to tap water. At sacrifice, mice were anesthetized with a ketamine/xylazine (100 mg*kg⁻¹/5 mg*kg⁻¹) cocktail via intraperitoneal injection. The euthanasia of all mice was carried out within two days. The experiments were performed in accordance with the approvals published by the Cantonal Committee on Animal Welfare [Amt für Landwirtschaft und Natur des Kantons Bern (27/12)] and the University of Bern.

Running wheel exercise

All mice were housed individually in cages each equipped with an 18 cm-diameter impeller purchased from a local pet shop (Fressnapf, Dietikon, Switzerland) and a magnetic revolution counter (in-house manufacturing with components obtained from Conrad, Dietikon, Switzerland). The revolution counters were read and reset to zero daily at 8:30 AM and 5 PM. For calculation of the running distances (in m), the number of rotations were multiplied by $2 * \pi * 0.09$ (the latter value is the radius of the impeller in m).

Chemical fixation

Plantaris muscle (PLNT) samples were chemically fixed in a 6.25% (v/v) glutaraldehyde solution buffered with 0.1 M sodium cacodylate-HCl (pH 7.4) and stored at 4°C until analysis.

Light microscopy and morphometry of capillarity

The chemically fixed PLNT samples were divided into 4-5 pieces, each with a volume of approximately 0.5 mm³, after which they were post-fixed in 1% (w/v) OsO₄, stained *en bloc* and embedded in Epon 812 (Fluka, Buchs, Switzerland).

One-micrometer 'semithin' sections were cut using a diamond knife and stained with 0.5% (w/v) Toluidine Blue dissolved in 1% (w/v) sodium tetraborate for 15 sec.

For the morphometric evaluation of capillarity, transverse sections through the muscle (size of approximately 1 mm²) were cut from two randomly selected Epon blocks from each PLNT. A systematic sampling strategy was implemented to acquire six light micrographs of each section at a magnification of x400 in a Leica DMR light microscope (Leica Microsystems, Heerbrugg, Switzerland). The light microscope was equipped with a programmable motor-driven x/y-sampling stage allowing defined stepwise movements to sample image fields in a systematic uniform random way. This equipment ensured that the micrographs, which we recorded for the morphometric analysis, embody non-overlapping areas representative for the entire muscle cross-section. Subsequently, the EPON blocks were turned 90° to prepare longitudinal sections, which were always large enough to gain six light micrographs taken by the same protocol mentioned above.

On the light micrographs of the transverse PLNT sections, the number of capillary profiles and that of muscle fiber profiles were counted taking into account the forbidden line rule (Weibel, 1979). The mean cross-sectional fiber area (MCSFA) was estimated by relating the area on the micrographs covered by skeletal muscle fiber profiles (which was assessed by point counting on a 10x10 point grid with each point representing an area of 0.365 μm²) to the number of muscle fiber profiles. The capillary-to-fiber (CF) ratio was computed as the number of capillary profiles divided by the number of skeletal muscle fibers, while the capillary (profile) density on transverse sections $N_{A(c,f)} = Q_A(0)$ was calculated as the number of capillary profiles divided by the section area covered by skeletal muscle fiber profiles.

The sarcomere length was determined on the longitudinal PLNT sections. Therefore, an at least 100 μm long reference line was drawn digitally along a muscle fiber profile orthogonal to the sarcomeric striation and in parallel to the sarcolemma. Densitometry was performed along this reference line to visualize the sarcomeric striation. The length of the reference line was related to the number of sarcomeric units in order to obtain the mean sarcomere length.

The dimension-less tortuosity factor on transverse sections $c(K,0)$ was established following a morphometric protocol developed by Weibel, Mathieu-Costello and colleagues (Mathieu et al., 1983; Mathieu-Costello et al., 1989). This procedure takes into account the 'Fisher axial distribution' for directional anisotropy. Therefore,

the ratio between the capillary density on the transverse sections $Q_A(0)$ and the capillary density on the longitudinal sections $Q_A(\pi/2)$ was calculated. $Q_A(0)/Q_A(\pi/2)$ can be used to read out the concentration parameter K and the corresponding tortuosity factor $c(K,0)$ in Mathieu et al., 1983. For reasons of simplicity, this procedure might be abbreviated by application of the polynomial function which we have developed by making use of the data collection published by Mathieu et al., 1983: $c(K,0) = -0.0011*x^5 + 0.0261*x^4 - 0.25*x^3 + 1.1709*x^2 - 2.7535*x + 3.7875$, with x standing for $Q_A(0)/Q_A(\pi/2)$. To our experiences, this equation results in acceptable approximations for the tortuosity factor in ranges for $Q_A(0)/Q_A(\pi/2)$ that exist in skeletal muscles of humans and rodents.

The capillary length density J_v was calculated by multiplication of the values for capillary density $Q_A(0)$ and the tortuosity factor $c(K,0)$.

Transmission electron microscopy

Ultrathin sections (50-60 nm in thickness) of the muscles were prepared with an Ultracut ultramicrotome (Reichert-Jung, Bensheim, Germany), floated on 200-mesh copper grids (Plano, Wetzlar, Germany) and contrasted with uranyl acetate and lead citrate. The inspection was carried out using a transmission electron microscope (TEM; Morgagni M268; FEI, Brno, Czech Republic).

Capillary morphometry

Twenty-twenty five randomly depicted electron micrographs of capillary profiles per ultrathin section were photographed in the TEM at a final magnification of $\times 7.800$. Micrographs showing capillary profiles with a length-to-width ratio of the smallest and the longest diameter of more than 1.2 were considered to be too obliquely or longitudinally sectioned and were thus excluded from morphometric evaluation.

Tablet-based image analysis (TBIA) was performed for the capillary morphometry by two researchers. On 20 electron micrographs showing the capillaries, lines were drawn with a digital pen around the lumen (lumen/EC-transition), along the abluminal EC surface (EC/BM-transition), at the BM/endomysium transition and around the PC surface of the capillaries. By processing with ImageJ, the values for the profile areas (A_{lumen} , A_{EC} , A_{PC} , A_{BM}) and profile perimeters ($P_{\text{lumen/EC}}$, $P_{\text{EC/BM transition}}$, $P_{\text{BM/endomysium transition}}$) of the structures of interest were obtained and then the means of the two measurements were computed to gain structural indicators that describe

quantitatively the capillary ultrastructure: the absolute cross-sectional area (A) of the capillary and each of its compartments, the profile area density (A_A) of each compartment relative to the capillary profile area ($A_{\text{lumen}}+A_{\text{EC}}+A_{\text{PC}}+A_{\text{BM}}$). The absolute values for the radius of the lumen and the total capillary profile as well as the arithmetic thickness (T) of the endothelium and the BM were calculated as previously reported (Bigler et al., 2016).

The PC coverage of capillaries was estimated as ratio of the length of the abluminal EC perimeter covered by a PC profile with the total abluminal EC perimeter, as previously reported (Egginton et al., 1996; Tilton et al., 1985). The intraluminal EC-surface enlargement was calculated as the length of the luminal EC perimeter with EC protrusions divided through luminal EC perimeter without protrusions minus 1. For additional characterization of intraluminal EC-surface enlargement we related the number of capillary profiles with intraluminal protrusions/filopodia longer than $5.2 \mu\text{m}$ to (which corresponds approximately to the doubled mean inner diameter of the capillaries) to the number of total capillary profiles.

The junctional interaction between ECs and PCs was assessed in accordance to previously reports (Allsopp and Gamble, 1979; Bigler et al., 2016; Egginton et al., 1996). Therefore, semi-quantitative indicators were computed by relating the number of capillary profiles exhibiting the subcompartmental junctions of interest (i.e. projections of the PCs ('PC pegs') invading the ECs ('EC sockets') as well as intracellular holes in PCs ('PC sockets') caused by invading EC projections ('EC pegs'), PC curling or PC-PC contacts) to the total number of capillary profiles analyzed.

Statistics

Numerical data are expressed as mean values together with the standard deviations. All morphometric data sets were tested by Kolmogorov-Smirnoff with Lilliefors-correction and Shapiro-Wilk for their normality of distribution prior statistical analysis. Comparisons pertaining to the morphometric analyses between control mice and mice of the 1wk-t and 6wks-t groups were checked using an one-way ANOVA followed by pairwise post-hoc Tukey's multiple comparison test. If the third value of a structural indicator (6wks-t) was inverting the trend of the second value (1wk-t), we additionally tested for statistical significance by performing pairwise two-tailed Student's T-test, as effects reversed by extended running wheel training

(discontinuous sequence) are not picked up by ANOVA. The levels of statistical significance in ANOVA $\alpha = 0.05$; Tukey's multiple comparison test $\alpha = 0.05$; 0.01 and 0.001, respectively, as well as Student's T-test $\alpha = 0.05$.

RESULTS

Running activity of the mice

The performance of the mice forming the 6-weeks training (6wks-t) group increased significantly during the second and third weeks of the training period (**Fig. 1**): their initial mean daily running distance of 5.3 ± 0.9 km improved 45% in the second week (compared to the first week) to rise additional 40% in the third week (compared to the second week). The changes in the daily running distance measured in the following weeks (5% in the 4th week, 17% in the 5th week and -3% in the 6th week; always in respect to the mean running distance of the previous week) were not significant. In total, the daily running distance of the mice increased 139% between the first and the sixth week of training. Taken together, the running activity of the mice improved for three weeks to merge into equilibrium at a high level for the residual training period. Impressively, some mice were active on the running wheel for approximately 18 km per day after 6 weeks of exercising. We also want to mention that the mice of the 1-week training (1wk-t) group ran daily 5.1 ± 0.8 km on the running wheel (data not shown) which corresponds to the first week running activity of the 6wks-t group.

Capillarity in the plantaris muscle

On transverse sections (**Fig. 2A,C,E**) of the plantaris muscle (PLNT), capillaries were identified as small round-shaped profiles mostly with visible lumen surrounding the skeletal muscle fiber profiles. On longitudinal sections (**Fig. 2B,D,F**), capillaries were distinguishable as round-shaped or oblique profiles (either isolated or grouped) that were elongated to a variable extent. The elongated capillary profiles appeared to preponderate in the PLNT of the mice from the control group (**Fig. 2B**), while the round-shaped capillary profiles were more frequently observed in the PLNT of the exercising mice (**Fig. 2D,F**), especially in the 6wks-t mice (**Fig. 2F**). Furthermore, a

regular striation was noticed inside the skeletal muscle fibers on the sections of all mice, which was caused by their sarcomeric organization (**Fig. 2F, inset**).

The transverse and longitudinal semithin sections of the PLNT were subjected to morphometry (**Fig. 3**). The capillary/fiber (CF)-ratio (32%; $P \leq 0.05$) and the capillary density $N_{A(c,f)}$ (36%; $P \leq 0.05$) were higher in the 1wk-t group than the control group. In the 6wks-t group, CF-ratio (34%; $P \leq 0.01$) and $N_{A(c,f)}$ (23%; $P = 0.07$) were likewise higher than in the 1wk-t group and, thus in total, 76% (CF-ratio; $P \leq 0.001$) and 66% ($N_{A(c,f)}$; $P \leq 0.001$) higher than in the control group. The mean cross-sectional muscle fiber area (MCSFA) and the sarcomere length varied only non-significantly between the three groups (MCSFA: control vs. 1wk-t: -6.3% / control vs. 6wks-t: + 2.3% / 1wk-t vs. 6wks-t: 9.2%; sarcomere length: control vs. 1wk-t: -1.6% / control vs. 6wks-t: -3.9% / 1wk-t vs. 6wks-t: -2.4%). The tortuosity factor $c(K,0)$ in the PLNT differed only non-significantly (6.7%) between the control and the 1wks-t groups and (9.0%) between the 1wk-t and 6wks-t groups. In total, $c(K,0)$ was significantly 16.3%-higher in the PLNT of the 6wks-t mice compared to the control group. The capillary length density J_v in the PLNT was significantly 43%-higher in the 1wk-t group than the control group and significantly 34%-higher in the 6wks-t group than in the 1wk-t group resulting in a significantly 92%-difference between the 6wks-t and the control group.

Capillary ultrastructure

While the transversely sectioned capillary profiles from the PLNT of mice from the three study groups (**Fig. 4A-C**) were subjected to a morphometric analysis for the quantitative assessment of their compartmental composition (lumen, endothelial cell (EC), basement membrane (BM) and pericyte (PC)), the longitudinally sectioned capillary profiles were studied only qualitatively. Strikingly, we occasionally found large series of transversely sectioned capillaries to be girded in sarcolemmal pits in close neighborhood to densely packed subsarcolemmal mitochondria (**Fig. 4D**). We furthermore used the transverse capillary sections to assess semi-quantitatively the appearance of sub-compartmental peg-socket junctions (PC-pegs/EC-socket; EC-pegs/PC-socket) in the PLNT of the mice from the three study groups. As seen in the examples shown in **Fig. 4E-I**, peg-socket junctions represent projections or filopodia of cells ('pegs') that curl into itself or invade other cells at their abluminal surface visible as pale pockets and holes in their cytoplasm ('sockets').

For each PLNT, electron micrographs of 20 randomly selected capillaries were subjected to morphometry. As shown in **Tab. 1**, the profile area size belonging to the capillary lumen A(lumen) was larger (30%, $P=0.06$, $P=0.04$ in Student's T-test) in the PLNT of 1wk-t mice than controls. The profile area density of the BM was lower (-19.8%; $P\leq 0.05$) after 1 week of training and (-20.7%; $P\leq 0.05$) after 6 weeks of training. Computation of the values for profile area sizes and perimeters revealed that the radius of the capillary lumen tended to be higher (17.6%; $P=0.09$, $P=0.03$ in Student's T-test) in the 1wk-t group than the control group, while the radius values of the 6wks-t group were between those of the control (13.2%; $P>0.05$) and 1wk-t (-3.8%; $P>0.05$) groups (**Fig. 5**). Interestingly, the BM thickness tended to be lower (-12.7%; $P=0.09$, $P=0.04$ in Student's T-test) in the 1wk-t group and was lower (-16.5%; $P\leq 0.05$) in the 6wks-t group than the control group suggesting that the running wheel training was accompanied by a continuous thinning of the pericapillary BM in absolute size.

Some structural indicators were semi-quantitatively analyzed. The PC coverage at the abluminal EC surface differed non-significantly between the mice of the three study groups (control vs. 1wk-t: -1.4%; control vs. 6wks-t: -3.0%; 1wk-t vs. 6wks-t: -4.3%). The relative enlargement of the intraluminal EC perimeters by protrusions was lower (-21% after 1-wk-t, -24% after 6 wks-t; $P\leq 0.05$) in the PLNT capillaries after the running wheel training than in the capillaries from the PLNT of the control animals. The percentage of PLNT capillary profiles with peg-socket junctions differed only non-significantly between the mice from the three study groups (EC-sockets: control vs. 1wk-t: $20.7 \pm 2.8\%$; control vs. 6wks-t: $19.4 \pm 6.5\%$, 1wk-t vs. 6wks-t: $16.7 \pm 6.7\%$; PC-sockets: control vs. 1wk-t: $3.0 \pm 4.5\%$, control vs. 6wks-t: $6.7 \pm 6.1\%$, 1wk-t vs. 6wks-t: $2.5 \pm 4.2\%$).

Remarkably, the values for profile area sizes, compartment perimeters and profile area densities of the capillaries from the PLNT of 6wks-t mice were between those of the control and 1wk-t groups (**Tab. 1**) suggesting that these changes in capillary structure established in the early phase reversed during the late phase of the training period. The coefficient of variation (CV) for all structural indicators differed 8.1%-26.8% being in the range of 20% for most indicators (data not shown).

Some structural peculiarities were discovered in capillaries depicted on the electron micrographs, which we describe here only qualitatively due to the low frequency of their occurrence (**Fig. 6**). Occasionally ($n = 4$ from 360 capillary profiles), capillary

profiles exhibited a second small lumen besides the major lumen (**Fig. 6A**). These branches might embody abluminal sprouts (characteristic of sprouting angiogenesis) but might alternatively represent tangentially sectioned or commencing branches of an established capillary. In some capillaries of the PLNT from mice of the three study groups, one or more very long EC protrusions projected into the capillary lumen (**Fig. 6B**). The proportion of capillary profiles with intraluminal protrusions/filopodia longer than 5.2 μm (which would be able to divide a capillary lumen into two approximately equal-sized openings if they were connected to the opposite capillary wall) differed significantly between the controls and the two exercise groups (controls: $19.4 \pm 11.4\%$; 1wk-t: $7.0 \pm 4.5\%$; 6wks-t: $2.0 \pm 6.1\%$). Once only, we noticed a clearly transversely sectioned muscle fiber, which was accompanied by an exactly orthogonally running capillary (**Fig. 6C**). Also singularly, a mysterious feature was seen on a micrograph, which could not be identified without doubt and probably represents a structural artifact generated by tissue shrinkage during the glutaraldehyde fixation (**Fig. 6D**).

DISCUSSION

In this investigation, we have characterized the running activity of C57BL/6 mice that were subjected to voluntary running wheel training for 1 week (1wk-t) or 6 weeks (6wks-t) in comparison to those of untrained littermates to subsequently assess morphometrically the capillarity and the ultrastructure of capillaries in the plantaris muscle (PLNT) of all mice. Essentially, we have made three major observations: 1. The mean daily running distance of the 6wks-t mice significantly increased after the initial training week for additional two weeks to establish a high-level equilibrium for the remaining three weeks of the running wheel training. 2. The higher CF-ratio in PLNT observed in the 6wks-t group compared to the controls was accompanied by a higher tortuosity factor $c(K,0)$ and a higher capillarity length density J_v . 3. The morphometric analysis of transmission electron micrographs revealed a tendency for lumen expansion of the capillaries in the 1wk-t group but not in the 6wks-t mice. The running wheel training of the mice was also accompanied by a continuous decrease in the pericapillary basement membrane thickness (CBMT) and shortening of intraluminal protrusions/filopodia.

The running activity of the 6wks-t mice was monitored throughout the training period. The statistical comparison revealed the daily running distance to be significantly increased only in the two weeks after the first training week. Thereafter, the mean daily running distance changed only non-significantly from week to week. Two other studies also report that C57BL/6 mice undergoing voluntary running wheel training showed increased activity for several weeks before persisting on a high level. In one study, the mice had already reached their maximum after 2 weeks (Waters et al., 2004), while the running distance increased over a time period of 4 weeks in the other study (Olenich et al., 2013). Although the reasons for the slightly varying kinetics of the running activity described in these reports are not known, it is possible that discrepancies in the impeller diameters (Waters et al: 11 cm; Olenich et al: 11.5 cm; our study: 18 cm) or differences in age of the mice when starting with training (Waters et al: 8 weeks; Olenich et al: not specified; our study: 12 weeks) contributed to these variations. However, all three studies are in agreement that mice cannot permanently improve their daily running performance but stabilize at a high level after several weeks of training. The two time points at which we collected muscle samples for structural analysis reflect this two-part kinetics: one group was derived from the phase of increasing running distance (after the first week of wheel training),

while the second group originated from the equilibrium phase of running activity (after six weeks of wheel training).

The capillary/fiber (CF)-ratio represents the most established structural indicator of capillarity in skeletal muscle, which is particularly used to provide experimental evidence for the occurrence of angiogenesis in this tissue (Hudlicka, 1998). The fact that the CF-ratio in PLNT of the 6wks-t group was significantly higher than in the control group indicates that physiological angiogenesis occurred in this period in response to long-term endurance exercise as previously demonstrated in humans (Andersen and Henriksson, 1977; Hoppeler et al., 1985) and rats (Olfert et al., 2001). Thus, endurance exercise is an effective trigger of angiogenesis (Egginton, 2009; Prior et al., 2004; Yan et al., 2011). Since the CF-ratio was higher in the 1wk-t group than the controls and in the 6wks-t group than the 1wk-t group, it can be assumed that the angiogenic process was continuously enduring throughout the training.

Because the CF-ratio is determined on transverse muscle sections, this indicator is representative only of the two-dimensional capillary arrangement but does not provide quantitative information about the isotropic (spatial) course of capillaries, e.g. caused by meandering capillaries with many anastomoses and/or branches. In contrast, the capillary length density (J_v), which represents an estimate of the total length of the capillaries within a defined tissue volume, is suitable to quantitatively describe the three-dimensional arrangement of the capillary system. For the evaluation of J_v , isotropic uniform random (IUR) sampling/sectioning according to classical stereological rules is formally the method of choice (Weibel, 1979). However, IUR on skeletal muscle is laborious to implement (Vock et al., 1996), because this stereological approach requires a large number of tissue sections that are not always available when analyzing muscle samples. Therefore, the dimensionless tortuosity factor was introduced as alternative to the analysis of IUR sections (Mathieu et al., 1983), which is calculated by relating the capillary density on transverse sections $Q_A(0)$ to that on longitudinal sections $Q_A(\pi/2)$. We would like to emphasize that discrepancies in the capillary tortuosity do not affect the CF-ratio to a significant extent. It should also be noted that other alternative methods for the estimation of capillary tortuosity have been developed (Gueugneau et al., 2016; Vincent et al., 2010), some of which are more laborious to carry out (Charifi et al., 2004; Janacek et al., 2011) than the protocol provided by Mathieu et al., 1983, which we have used in the present study. The tortuosity factor is characteristic of any

muscle, species and preparation method (Mathieu-Costello et al., 1989) but is not significantly affected by parameters such as body size, aerobic capacity and hypoxia (Mathieu-Costello et al., 1989) as well as by endurance exercise in the oxidative soleus muscle of rats (Poole and Mathieu-Costello, 1989). However, the tortuosity factor is related to the sarcomere length in the muscle (Mathieu-Costello, 1987).

In our study, the tortuosity factor was significantly higher in the PLNT of the 6wks-t group than the controls indicating that the three-dimensional arrangement of the capillary network in this glycolytic muscle has changed during the training period by becoming more convoluted. We suggest that the increase in capillary tortuosity extends the diffusion capacity of oxygen/carbon dioxide and energy substrates, thereby contributing to the fiber shifting towards a more oxidative phenotype induced by endurance training (Freysenet, 2007; Hood et al., 2006). Consistent with this hypothesis, an increase in capillary tortuosity was found to be related to the activity of oxidative enzymes in skeletal muscle fibers after 14 weeks of moderate ergometer training (Charifi et al., 2004). In addition, a computer simulation revealed that an increase in capillary tortuosity in skeletal muscle causes a higher tissue oxygenation, particularly when combined with anastomoses (Goldman and Popel, 2000). However, the mechanisms how endurance exercise triggers an increase in capillary tortuosity, are not known. It has previously been speculated (Egginton et al., 2001) that the high rates of EC stretching during training result in elongation of the capillaries, so that they meander, as it has been observed by intravital microscopy (Ellis et al., 1990).

To the best of our knowledge, this is the first study in which the ultrastructural phenotype of capillaries in skeletal muscle of mice has been evaluated after endurance exercise. Because the PLNT of the mice were prepared one day after the last training session, the ultrastructural changes of the here described capillaries, were not acutely caused by the higher contractility but represent chronic adjustments in the capillary phenotype, instead.

The profile area sizes associated with the capillary lumen in the PLNT tended to be larger in the 1wk-t mice than in the controls. Correspondingly, the luminal capillary radius tended to be higher in the 1wk-t than the untrained mice. These findings indicate that the running wheel training resulted in the expansion of the capillary lumen after the first week of training, which could be due to exercise-induced higher cardiac output that increases blood flow through the capillaries in the periphery

(Hellsten and Nyberg, 2016). After six weeks of training, the profile area size of the capillary lumen was again lower (but did not reach the baseline values). Obviously, the lumen-related structural adaptation of the capillary was reversed after the long-lasting training stimulus. It is therefore tempting to speculate that the blood flow is better distributed through the capillaries in the PLNT after angiogenesis has occurred, which in turn reduces the wall stress in capillaries, resulting in a lower lumen diameter (Masuda et al., 2003).

The pericapillary BM thickness (CBMT) was significantly reduced as well as the sizes and numbers of the intraluminal protrusion were lower in the 1wk-t group than in the control group and then again lower in the 6wks-t group. These findings suggest that the running wheel training of the mice was accompanied by a continuous thinning of the CBMT and a reduction in the intraluminal protrusion surface of their PLNT capillaries over time. A decrease of the CBMT in skeletal muscle after endurance exercise of humans was likewise observed in other studies (Baum and Bigler, 2016; Williamson et al., 1996). On the other hand, several potential triggers and causes for the increase of the CBMT, such as increased hydrostatic pressure, reduction in blood flow, more glycation events and chronic inflammation have been identified (Baum and Bigler, 2016). Whether the exercise-induced change(s) in extent of one or more of these triggers of CBMT thickening contribute(s) to the reversible response observed in this study, meaning the CBMT thinning, is an interesting issue that should be investigated in further studies.

Because it appeared likely to us that endurance exercise causes only temporal changes in the capillary ultrastructure, we have tested for statistical significances of our measurements by both formally correct ANOVA as well as pairwise Student's T-test. The calculations showed that a few structural indicators only tended to vary between the study groups when applying ANOVA, while they significantly differed in the Student's T-test: the capillary (profile) density $N_{A(c,f)}$ between the 1-wk-t and 6-wks-t groups, the area size of the capillary lumen between the controls and both the 1-wk-t and the 6-wks-t groups and the CBMT between the controls and 1-wk-t group. It is currently not possible to decide which of these differences in capillary structure are actually significant because they represent reversal adaptations of the microvasculature.

Taken together, the training-dependent changes in lumen and BM appearance in murine skeletal muscle capillaries described in this study are consistent to those observed in human skeletal muscle after endurance exercise. In contrast, increase of PC coverage was only observed in skeletal muscle capillaries of humans (Baum et al., 2015) but not in those of mice as shown here. Whether this distinction represents a species-specific difference in the structural adaptation of capillaries to exercise is an open question.

In skeletal muscle of rodents, several features of changes in the capillary phenotype characteristic of splitting and sprouting angiogenesis have been identified (Egginton, 2009; Egginton et al., 2001; Hudlicka, 1998). During splitting angiogenesis, a higher proportion of intraluminal irregularities, projections and septa combined with extensive cytoplasmic vacuolization of ECs were observed in skeletal muscle capillaries of prazosin-treated rats compared to those of control animals (Egginton et al., 2016; Zhou et al., 1998a). Sprouting angiogenesis in skeletal muscle of rats induced by surgical extirpation of a synergistic muscle was associated with an increase of abluminal EC processes, a higher PC coverage of capillaries, higher rates of EC mitosis and focal breakage of the pericapillary BM (Hudlicka, 1998; Zhou et al., 1998b). If these structural hallmarks for splitting and sprouting angiogenesis (prazosin model, overload model) are compared to the morphometric findings described in the present investigation, a dissenting picture emerges. Neither of the splitting nor sprouting angiogenesis-related findings mentioned above were observed in our study. Thus, it is yet not possible to make a statement about the mode by which physiological angiogenesis is realized in skeletal muscles of mice in response to endurance exercise. (Yan et al., 2011)

We are aware that some methodological limitations may restrict the significance of our findings: 1. Although we are not able to make a statement about the running activities of the trained mice and their untrained control littermates, we consider this issue to be negligible due to long recorded distance that the mice have trained on the running wheel. 2. We cannot exclude a technical bias during tissue treatment (e.g. shrinkage by glutaraldehyde fixation), but like to underline that all samples/sections were treated in the same way. However, it should be borne in mind that the values for the structural indicators presented here are not to be considered absolutely. 3. The capillary phenotype, even within a defined muscle, is highly

variable, e.g. most structural indicators show coefficient of variations (CVs) of about 20%. Thus, it is necessary to include a sufficient number of capillary profiles in the morphometric analysis. We used 360 micrographs of capillaries in our study (120 per group), which appears to be a sufficient number, while a number of 6-17 capillaries per study group is certainly too low (Uchida et al., 2015) and may lead to wrong conclusions and interpretations of the outcome. 4. Arithmetic values as provided in this study represent only structural estimates. For a more functional interpretation of the morphometric findings, such as their potential relationship to oxygen and substrate supply, other indicators are more appropriate: For example, the harmonic mean barrier thickness (Weibel, 1979), which takes into account the fact that thinner segments contribute more to diffusion than thicker ones in a proportional fashion. In summary, our morphometric study performed at the light microscopy and electron microscopy levels revealed both the capillarity and the capillary ultrastructure in PLNT to change over time during long-term endurance exercise training. In the early phase of the training period, angiogenesis and a tendency of capillary lumen expansion was accompanied by a significant reduction in CBMT and a shortening of mean intraluminal protrusion length and number. After long-term training, when the mice reached a steady state in running activity, additional angiogenesis and an increase in capillary tortuosity was established, which was accompanied by a partial reversal of the lumen expansion as well as further reductions in CBMT and shortening of the intraluminal protrusion length. The knowledge of these non-designed structural adjustments in the capillary phenotype may support the understanding of the changes in functionality of the microvasculature in response to endurance exercise, especially if these training-induced microvascular remodeling manifestations are regarded as control parameters in the negative feedback control circuit.

Acknowledgements

We would like to thank Christoph Lehmann, Bern very much for his excellent technical support in assembling und maintaining the running wheel equipment. Thanks to Anna Stocker for proof-reading of the manuscript. The assistance of Barbara Krieger to improve the graphical presentation is likewise highly appreciated.

GRANTS

This work was financially supported by a Swiss National Science Foundation Grant (320030-144167) to O. Baum.

DISCLOSURES

No conflicts of interest, financial or otherwise, are declared by the author(s).

REFERENCES

- Allsopp, G. and Gamble, H. J.** (1979). An electron microscopic study of the pericytes of the developing capillaries in human fetal brain and muscle. *J Anat* **128**, 155-168.
- Andersen, P. and Henriksson, J.** (1977). Capillary supply of the quadriceps femoris muscle of man: adaptive response to exercise. *J Physiol* **270**, 677-690.
- Baum, O. and Bigler, M.** (2016). Pericapillary basement membrane thickening in human skeletal muscles. *Am J Physiol Heart Circ Physiol* **311**, H654-666.
- Baum, O., Gubeli, J., Frese, S., Torchetti, E., Malik, C., Odriozola, A., Graber, F., Hoppeler, H. and Tschanz, S. A.** (2015). Angiogenesis-related ultrastructural changes to capillaries in human skeletal muscle in response to endurance exercise. *J Appl Physiol* (1985) **119**, 1118-1126.
- Bigler, M., Koutsantonis, D., Odriozola, A., Halm, S., Tschanz, S. A., Zakrzewicz, A., Weichert, A. and Baum, O.** (2016). Morphometry of skeletal muscle capillaries: the relationship between capillary ultrastructure and ageing in humans. *Acta Physiol (Oxf)* **218**, 98-111.
- Charifi, N., Kadi, F., Feasson, L., Costes, F., Geysant, A. and Denis, C.** (2004). Enhancement of microvessel tortuosity in the vastus lateralis muscle of old men in response to endurance training. *J Physiol* **554**, 559-569.
- Egginton, S.** (2009). Invited review: activity-induced angiogenesis. *Pflugers Arch* **457**, 963-977.
- Egginton, S. and Hudlicka, O.** (1999). Early changes in performance, blood flow and capillary fine structure in rat fast muscles induced by electrical stimulation. *J Physiol* **515 (Pt 1)**, 265-275.
- Egginton, S., Hudlicka, O., Brown, M. D., Graciotti, L. and Granata, A. L.** (1996). In vivo pericyte-endothelial cell interaction during angiogenesis in adult cardiac and skeletal muscle. *Microvasc Res* **51**, 213-228.
- Egginton, S., Hussain, A., Hall-Jones, J., Chaudhry, B., Syeda, F. and Glen, K. E.** (2016). Shear stress-induced angiogenesis in mouse muscle is independent of the vasodilator mechanism and quickly reversible. *Acta Physiol (Oxf)* **218**, 153-166.
- Egginton, S., Zhou, A. L., Brown, M. D. and Hudlicka, O.** (2001). Unorthodox angiogenesis in skeletal muscle. *Cardiovasc Res* **49**, 634-646.

Ellis, C. G., Mathieu-Costello, O., Potter, R. F., MacDonald, I. C. and Groom, A. C. (1990). Effect of sarcomere length on total capillary length in skeletal muscle: in vivo evidence for longitudinal stretching of capillaries. *Microvasc Res* **40**, 63-72.

Freysenet, D. (2007). Energy sensing and regulation of gene expression in skeletal muscle. *J Appl Physiol* (1985) **102**, 529-540.

Goldman, D. and Popel, A. S. (2000). A computational study of the effect of capillary network anastomoses and tortuosity on oxygen transport. *J Theor Biol* **206**, 181-194.

Gueugneau, M., Coudy-Gandilhon, C., Meunier, B., Combaret, L., Taillandier, D., Polge, C., Attaix, D., Roche, F., Feasson, L., Barthelemy, J. C. et al. (2016). Lower skeletal muscle capillarization in hypertensive elderly men. *Exp Gerontol* **76**, 80-88.

Hellsten, Y. and Nyberg, M. (2016). Cardiovascular adaptations to exercise training. *Compr Physiol* **6**, 1-32.

Holloszy, J. O. (1975). Adaptation of skeletal muscle to endurance exercise. *Med Sci Sports* **7**, 155-164.

Hood, D. A., Irrcher, I., Ljubicic, V. and Joseph, A. M. (2006). Coordination of metabolic plasticity in skeletal muscle. *J Exp Biol* **209**, 2265-2275.

Hoppeler, H., Baum, O., Lurman, G. and Mueller, M. (2011). Molecular mechanisms of muscle plasticity with exercise. *Comprehensive Physiology* **1**, 1383-1412.

Hoppeler, H., Howald, H., Conley, K., Lindstedt, S. L., Claassen, H., Vock, P. and Weibel, E. R. (1985). Endurance training in humans: aerobic capacity and structure of skeletal muscle. *J Appl Physiol* **59**, 320-327.

Hudlicka, O. (1998). Is physiological angiogenesis in skeletal muscle regulated by changes in microcirculation? *Microcirculation* **5**, 7-23.

Janacek, J., Cvetko, E., Kubinova, L., Travnik, L. and Erzen, I. (2011). A novel method for evaluation of capillarity in human skeletal muscles from confocal 3D images. *Microvasc Res* **81**, 231-238.

Laughlin, M. H. (2016). Physical activity-induced remodeling of vasculature in skeletal muscle: role in treatment of type 2 diabetes. *J Appl Physiol* (1985) **120**, 1-16.

Leick, L., Hellsten, Y., Fentz, J., Lyngby, S. S., Wojtaszewski, J. F., Hidalgo, J. and Pilegaard, H. (2009). PGC-1 α mediates exercise-induced

skeletal muscle VEGF expression in mice. *Am J Physiol Endocrinol Metab* **297**, E92-103.

Masuda, H., Kawamura, K., Nanjo, H., Sho, E., Komatsu, M., Sugiyama, T., Sugita, A., Asari, Y., Kobayashi, M., Ebina, T. et al. (2003). Ultrastructure of endothelial cells under flow alteration. *Microsc Res Tech* **60**, 2-12.

Mathieu, O., Cruz-Orive, L. M., Hoppeler, H. and Weibel, E. R. (1983). Estimating length density and quantifying anisotropy in skeletal muscle capillaries. *J Microsc* **131**, 131-146.

Mathieu-Costello, O. (1987). Capillary tortuosity and degree of contraction or extension of skeletal muscles. *Microvasc Res* **33**, 98-117.

Mathieu-Costello, O., Hoppeler, H. and Weibel, E. R. (1989). Capillary tortuosity in skeletal muscles of mammals depends on muscle contraction. *J Appl Physiol* **66**, 1436-1442.

Olenich, S. A., Gutierrez-Reed, N., Audet, G. N. and Olfert, I. M. (2013). Temporal response of positive and negative regulators in response to acute and chronic exercise training in mice. *J Physiol* **591**, 5157-5169.

Olfert, I. M., Baum, O., Hellsten, Y. and Egginton, S. (2016). Advances and challenges in skeletal muscle angiogenesis. *Am J Physiol Heart Circ Physiol* **310**, H326-336.

Olfert, I. M., Breen, E. C., Mathieu-Costello, O. and Wagner, P. D. (2001). Skeletal muscle capillarity and angiogenic mRNA levels after exercise training in normoxia and chronic hypoxia. *J Appl Physiol* (1985) **91**, 1176-1184.

Peeze Binkhorst, F. M., Kuipers, H., Heymans, J., Frederik, P. M., Slaaf, D. W., Tangelder, G. J. and Reneman, R. S. (1989). Exercise-induced focal skeletal muscle fiber degeneration and capillary morphology. *J Appl Physiol* (1985) **66**, 2857-2865.

Pette, D. and Staron, R. S. (1997). Mammalian skeletal muscle fiber type transitions. *Int Rev Cytol* **170**, 143-223.

Poole, D. C. and Mathieu-Costello, O. (1989). Skeletal muscle capillary geometry: adaptation to chronic hypoxia. *Respir Physiol* **77**, 21-29.

Prior, B. M., Yang, H. T. and Terjung, R. L. (2004). What makes vessels grow with exercise training? *J Appl Physiol* (1985) **97**, 1119-1128.

Tilton, R. G., Faller, A. M., Burkhardt, J. K., Hoffmann, P. L., Kilo, C. and Williamson, J. R. (1985). Pericyte degeneration and acellular capillaries are increased in the feet of human diabetic patients. *Diabetologia* **28**, 895-900.

Uchida, C., Nwadozi, E., Hasanee, A., Olenich, S., Olfert, I. M. and Haas, T. L. (2015). Muscle-derived vascular endothelial growth factor regulates microvascular remodelling in response to increased shear stress in mice. *Acta Physiol (Oxf)* **214**, 349-360.

Vincent, L., Feasson, L., Oyono-Enguelle, S., Banimbek, V., Denis, C., Guarneri, C., Aufradet, E., Monchanin, G., Martin, C., Gozal, D. et al. (2010). Remodeling of skeletal muscle microvasculature in sickle cell trait and alpha-thalassemia. *Am J Physiol Heart Circ Physiol* **298**, H375-384.

Vock, R., Weibel, E. R., Hoppeler, H., Ordway, G., Weber, J. M. and Taylor, C. R. (1996). Design of the oxygen and substrate pathways. V. Structural basis of vascular substrate supply to muscle cells. *J Exp Biol* **199**, 1675-1688.

Waters, R. E., Rotevatn, S., Li, P., Annex, B. H. and Yan, Z. (2004). Voluntary running induces fiber type-specific angiogenesis in mouse skeletal muscle. *Am J Physiol Cell Physiol* **287**, C1342-1348.

Weibel, E. (1979). *Stereological methods. Practical methods for biological morphometry*: London: Academic Press.

Williamson, J. R., Hoffmann, P. L., Kohrt, W. M., Spina, R. J., Coggan, A. R. and Holloszy, O. (1996). Endurance exercise training decreases capillary basement membrane width in older nondiabetic and diabetic adults. *J Appl Physiol* **80**, 747-753.

Yan, Z., Okutsu, M., Akhtar, Y. N. and Lira, V. A. (2011). Regulation of exercise-induced fiber type transformation, mitochondrial biogenesis, and angiogenesis in skeletal muscle. *J Appl Physiol* (1985) **110**, 264-274.

Zhou, A., Egginton, S., Hudlicka, O. and Brown, M. D. (1998a). Internal division of capillaries in rat skeletal muscle in response to chronic vasodilator treatment with alpha1-antagonist prazosin. *Cell Tissue Res* **293**, 293-303.

Zhou, A. L., Egginton, S., Brown, M. D. and Hudlicka, O. (1998b). Capillary growth in overloaded, hypertrophic adult rat skeletal muscle: an ultrastructural study. *Anat Rec* **252**, 49-63.

Figures

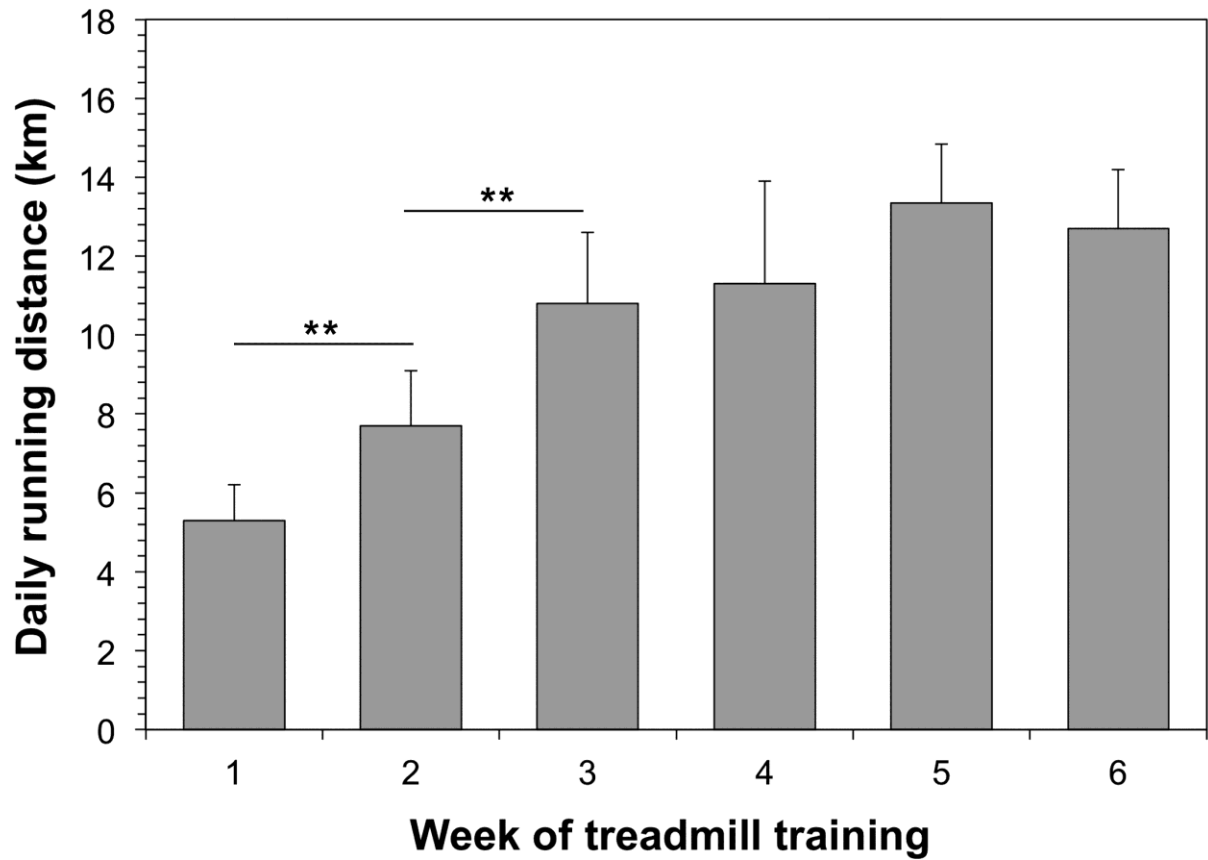


Figure 1: Running activity of C57BL/6-mice during six weeks of voluntary running wheel training. The running distance of each mouse was daily monitored and then used for calculation of the weekly performance. Shown are the means \pm standard deviations; $n=7$. **: $P \leq 0.01$ compared to the performance measured one week before.

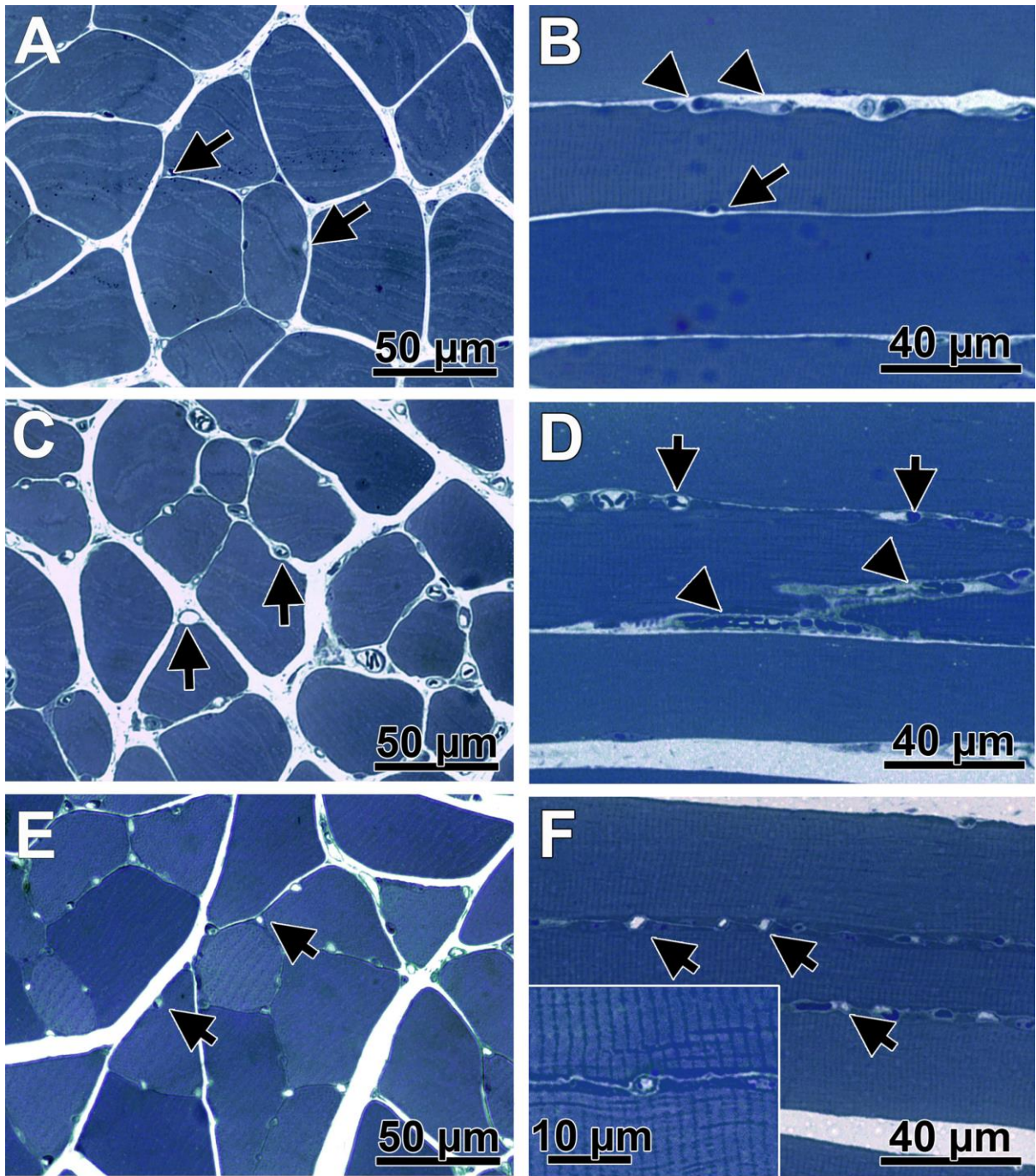


Figure 2: Representative light micrographs of toluidine blue-stained 1- μm -thick ('semithin') transverse (A,C,E) and longitudinal (B,D,F) sections of the plantaris muscle. A,B: control mouse; C,D: mouse after 1 week of running wheel training; E,F: mouse after 6 weeks of running wheel training. A,C,E: Note the capillary profiles (black arrows) in the endomysium surrounding the muscle fibers,

which appear with largest lumen in the PLNT of the mice trained for 1 week. **B,D,F:** Note round-shaped (black arrows) and elongated (arrowheads) capillary profiles as well as sarcomere-caused striation (insert in image F) of the skeletal muscle fibers. The dense sequence of the round-shaped capillary profiles in the plantaris muscle occasionally after 1 week and frequently after 6 weeks of running wheel training indicates an increased degree of capillary tortuosity.

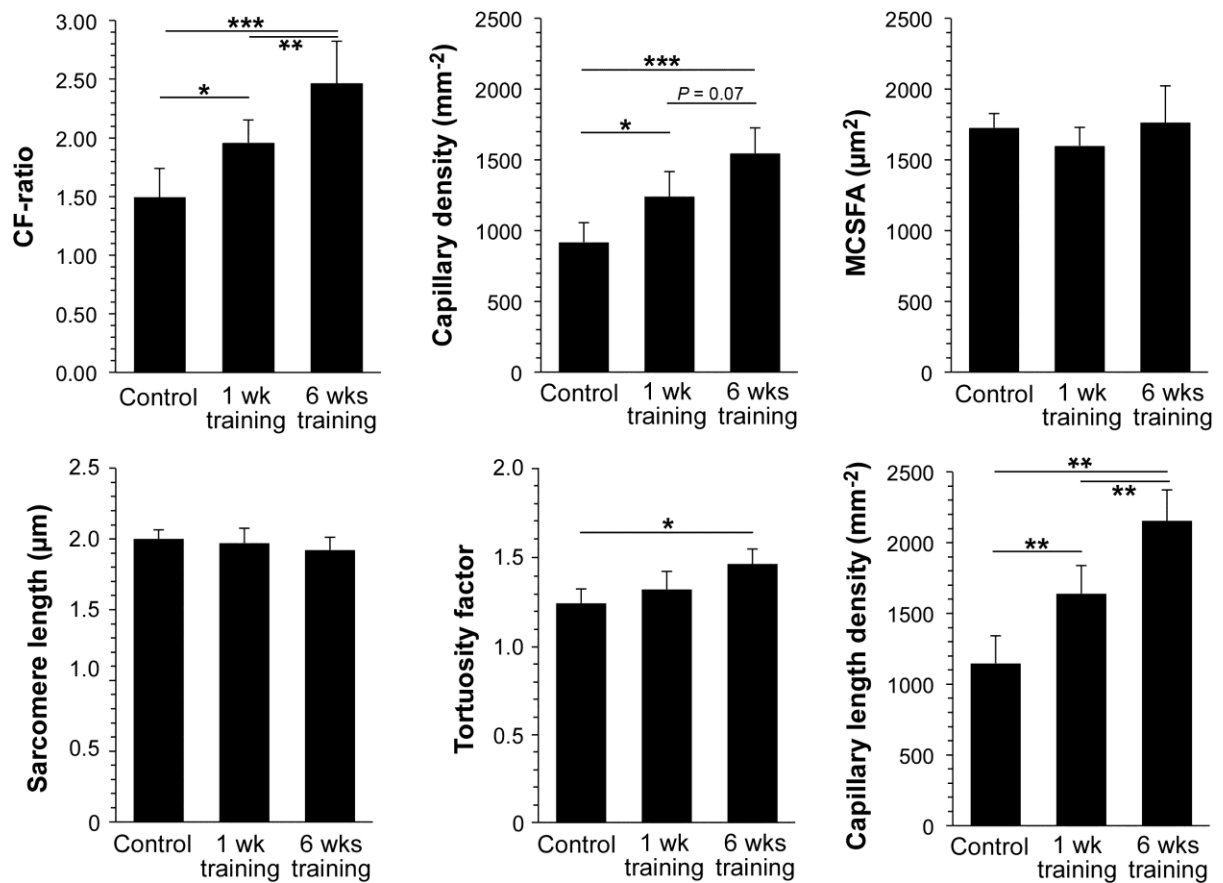


Figure 3: Capillarity in the plantaris muscle of untrained mice and mice undergoing voluntary running wheel training. Sarcomere distances, mean cross-sectional fiber area (MCSFA) and the numbers of muscle fiber and capillary profiles were quantified on light micrographs of transverse and longitudinal semithin sections by means of morphometry to subsequently compute the six indicators characteristic of the capillary phenotype in muscular tissue (CF-ratio, capillary density $N_{A(c,f)}$, MCSFA, sarcomere length, tortuosity factor $c(K,0)$ and capillary length density J_v). Mean values \pm standard deviations are shown. $n=5$ (control mice), 6 (1-week-trained mice) and 7 (6-weeks trained mice). *: $P \leq 0.05$, **: $P \leq 0.01$, ***: $P \leq 0.001$ in one-way ANOVA followed by pairwise post-hoc Tukey's multiple comparison testing.

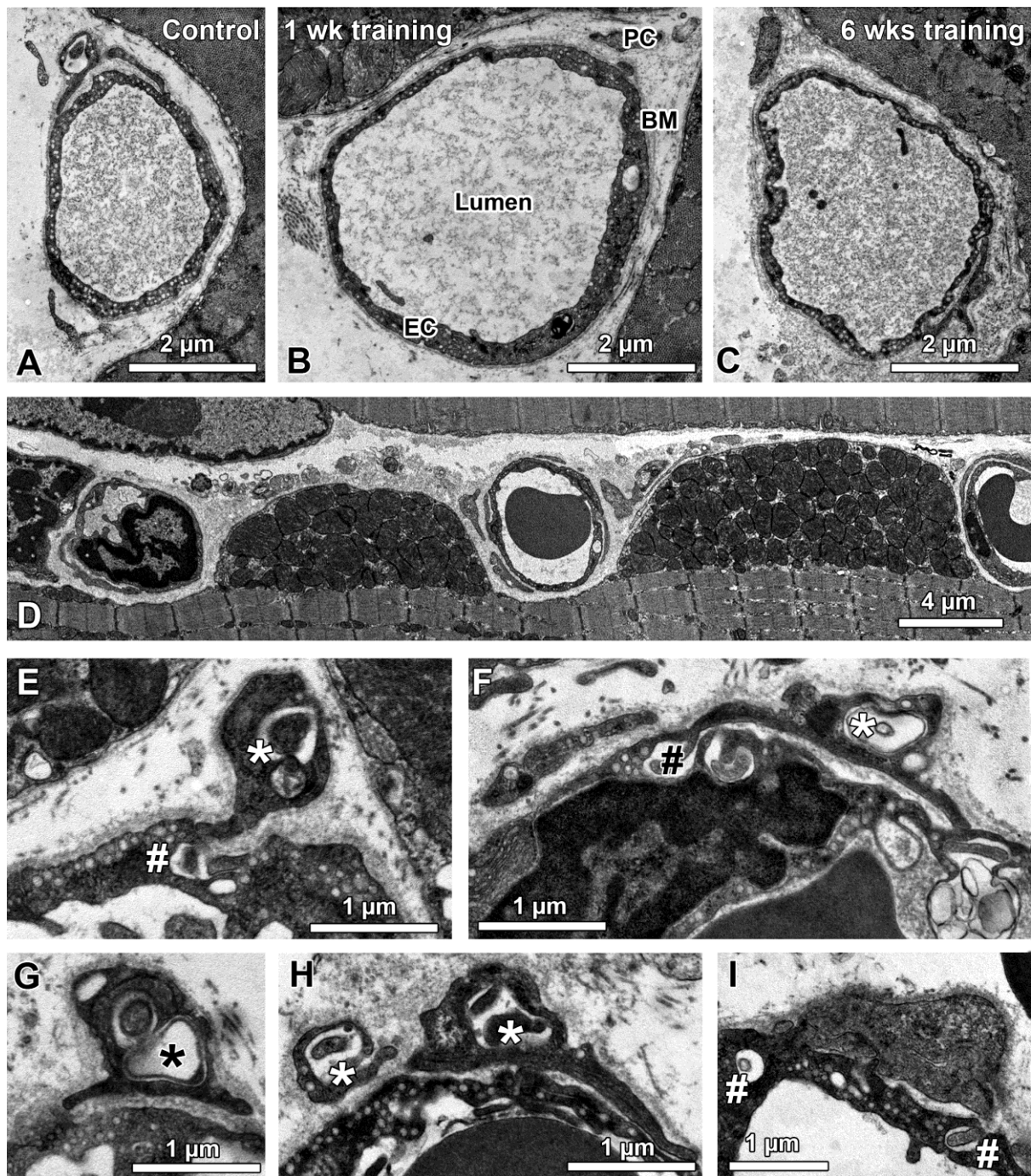


Figure 4: Transmission electron microscopy for the depiction of the capillary ultrastructure in plantaris muscle. A-C: Representative electron micrographs of transversely sectioned capillary profiles from plantaris muscle of a control mouse (A) and mice undergoing voluntary running wheel training for 1 week (B) or 6 weeks (C). The capillary compartments (lumen, endothelial cell (EC), basement membrane (BM)

and pericyte (PC)) are labeled in image B. Note that the images were recorded with the same magnification. **D:** On longitudinal sections of the plantaris muscle from mice (especially in those undergoing running wheel training), series of cross-sectioned capillary profiles were occasionally girded in sarcolemmal pits in close neighborhood to densely packed subsarcolemmal mitochondria indicating a highly tortuous course of the corresponding capillary sections. **E-I:** Sub-compartmental peg–socket junctions in capillaries. In PC profiles, empty or filled cytoplasmic holes (sockets) may be detected (* in images E-H). Correspondingly, EC sockets may be present in EC profiles (# in images E, F, I,) being evoked by invading PC pegs.

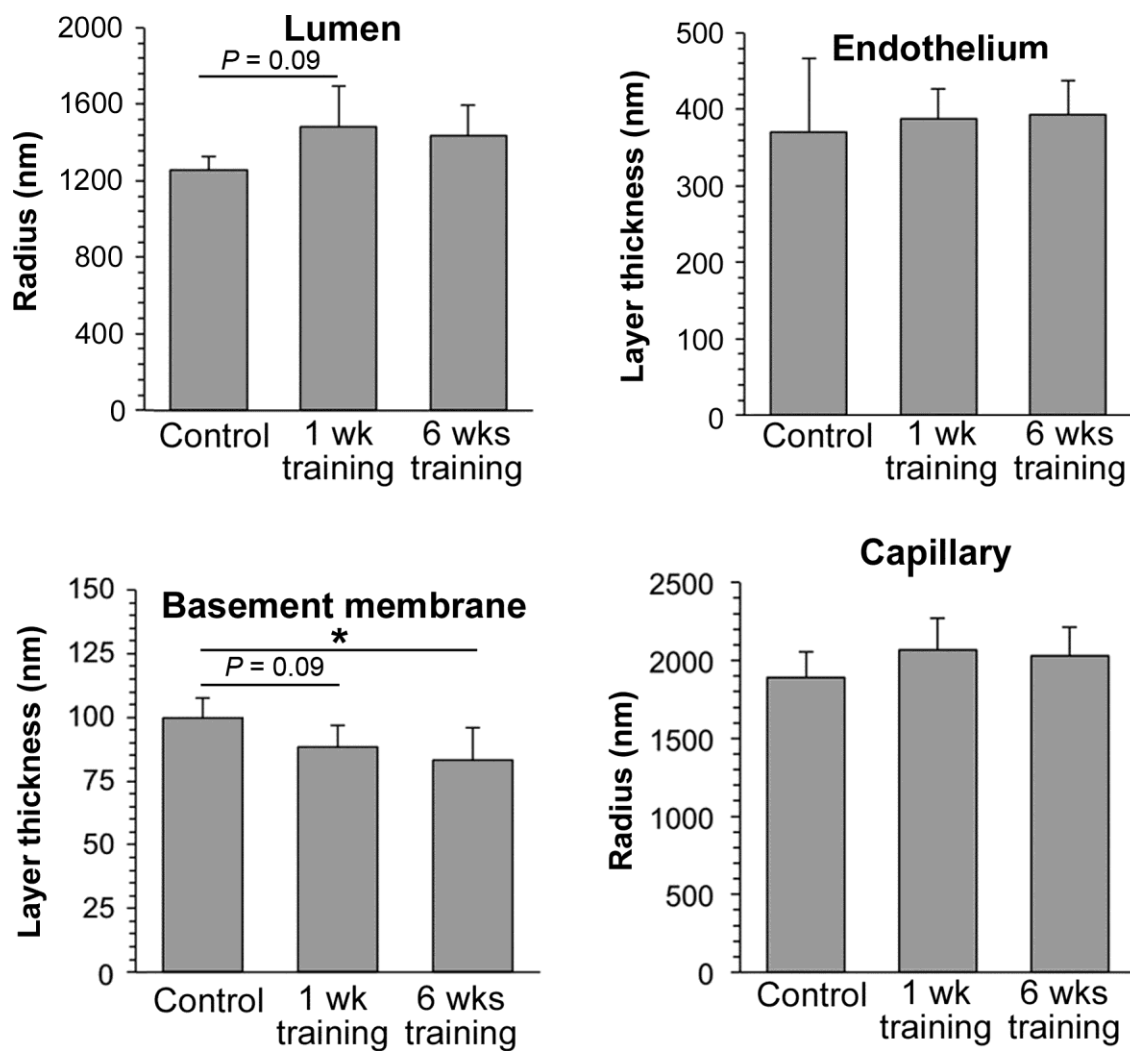


Figure 5: Morphometric determination of the thicknesses and the radius of the capillary compartments in mice remaining untrained or undergoing running wheel training for 1 week or 6 weeks. Tablet-based image analysis was applied to electron micrographs of capillaries from the plantaris muscle to measure areas and perimeters of the compartments with which morphometric indicators were computed. Means \pm standard deviations are shown; $n = 5$ (control mice), 6 (1-week-trained mice) and 7 (6-weeks trained mice). *: $P \leq 0.05$ in ANOVA followed by pairwise post-hoc Tukey's multiple comparison testing.

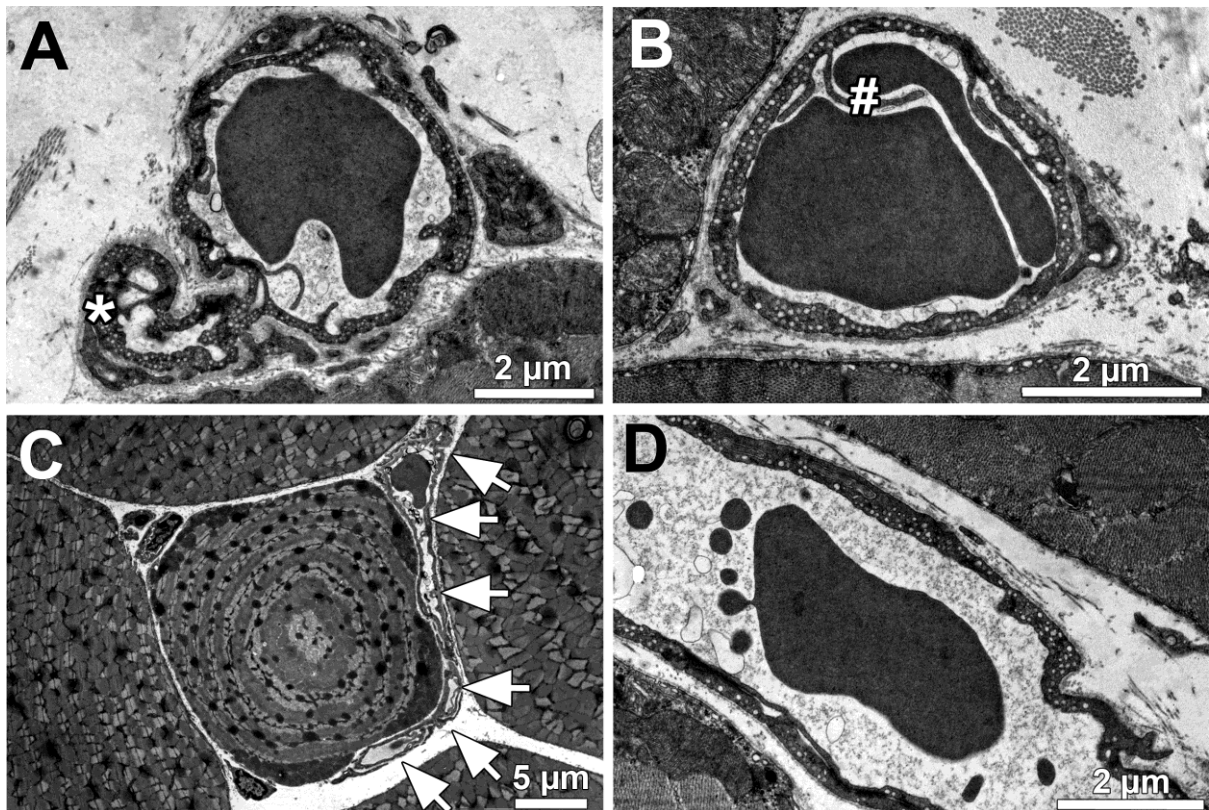


Figure 6: Ultrastructural peculiarities of capillaries noticed in the plantaris muscle of mice from this study. Transmission electron microscopy analysis revealed the manifestation of specific capillary features partially of functional relevance and thus interesting for readers. **A:** * Possible sprout or branch of a capillary, **B:** # Intraluminal EC protrusion in close contact to one or two erythrocyte(s), **C:** A transversely sectioned muscle fiber is accompanied by an orthogonally running capillary (arrows) substantiating the tortuous course of the capillary and **D:** Big Foot left a trace in a capillary lumen. A and C are examples derived from mice of the 6-weeks running wheel training group, while B and D are derived from a control mouse.

Table 1: Summary of the morphometric analysis to characterize the capillary phenotype in murine skeletal muscle induced by voluntary running wheel training. Transmission electron micrographs of the capillaries from plantaris muscle of mice from the 1-week training, 6-weeks training and control groups were subjected to morphometry by tablet-based image analysis to compute the listed structural indicators. Means \pm standard deviations are represented; n= 5 (control mice), 6 (1-week-trained mice) and 7 (6-weeks trained mice). Abbreviations: A = area; A_A = area density; P = perimeter; EC = endothelial cell; PC = pericyte; BM = basement membrane. ANOVA with Tukey post-hoc test and two-tailed Student's t-test statistics: 1 = control versus 1 week training; 2 = controls versus 6 weeks training; 3 = 1 wk training versus 6 wks training; NS (not significant) = $P > 0.05$; * = $P \leq 0.05$; ** = $P \leq 0.01$; ND = not determined.

	Control	1 week training	6 weeks training	ANOVA	Student's t-Test
A (lumen), μm^2	7.1 \pm 0.9	9.2 \pm 1.7	8.7 \pm 1.4	1:P=0.06	1:*,2:*
A (EC), μm^2	4.5 \pm 1.8	5.2 \pm 0.9	5.2 \pm 1.1	NS	ND
A (BM), μm^2	2.4 \pm 0.5	2.6 \pm 0.5	2.2 \pm 0.4	NS	NS
A (PC), μm^2	0.8 \pm 0.1	0.9 \pm 0.3	0.7 \pm 0.1	3:P=0.06	3:*
A (cap), μm^2	14.6 \pm 1.3	15.9 \pm 2.9	15.3 \pm 1.3	NS	NS
A_A (lumen; cap), %	51.2 \pm 5.6	54.3 \pm 3.6	55.0 \pm 4.9	NS	ND
A_A (EC; cap), %	31.1 \pm 5.7	30.1 \pm 2.7	30.8 \pm 3.9	NS	NS
A_A (BM; cap), %	12.5 \pm 0.8	10.0 \pm 1.2	9.9 \pm 1.4	1:**,2:**	ND
A_A (PC; cap), %	5.2 \pm 0.5	5.5 \pm 1.2	4.3 \pm 0.5	3:*	ND
P (lumen), μm	10.9 \pm 1.1	12.0 \pm 1.0	11.8 \pm 1.2	NS	NS
P (abluminal EC surface), μm	13.1 \pm 1.5	14.4 \pm 1.1	14.0 \pm 1.2	NS	NS
P (BM/endomysium transition), μm	14.6 \pm 1.3	15.9 \pm 1.2	15.3 \pm 1.3	NS	NS
Pericyte coverage, %	19.6 \pm 2.4	19.4 \pm 2.3	18.8 \pm 1.5	NS	ND
Luminal EC-surface enlargement by protrusion, %	22.6 \pm 2.9	17.8 \pm 3.2	17.2 \pm 2.1	1:*,2:*	ND
Capillary profiles with EC-sockets, %	20.7 \pm 2.8	19.4 \pm 6.5	16.7 \pm 6.7	NS	ND
Capillary profiles with PC-sockets, %	3.0 \pm 4.5	6.7 \pm 6.1	2.5 \pm 4.2	NS	NS